MoEDAL physics results and future plans

Vasiliki A. Mitsou[*] **on behalf of the MoEDAL Collaboration**
Instituto de Física Corpuscular (IFIC), CSIC – Universitat de València,
C/ Catedrático José Beltrán 2, E-46980 Paterna (Valencia), Spain
E-mail: vasiliki.mitsou@ific.uv.es

The MoEDAL experiment at the LHC is optimised to detect highly ionising particles (HIPs) such as magnetic monopoles, dyons and (multiply) electrically charged stable massive particles predicted in various theoretical scenarios. It combines (passive) nuclear track detectors with HIP trapping volumes. The detector concept and its physics reach is presented here with emphasis given to the recent result of monopole search considering pair production via photon fusion and to future prospects for searches for supersymmetry. Current and future detector extensions are also discussed.

Corfu Summer Institute 2019 "School and Workshops on Elementary Particle Physics and Gravity"
(CORFU2019)
31 August - 25 September 2019
Corfu, Greece

---

[*]Speaker.

1. Introduction

The MoEDAL (Monopole and Exotics Detector at the LHC) [1, 2] experiment at the Large Hadron Collider (LHC) [3] is dedicated to searches for manifestations of new physics through highly ionising particles in a manner complementary to ATLAS and CMS [4]. The most important motivation for the MoEDAL experiment is to pursue the quest for magnetic monopoles and dyons at LHC energies. In addition, the experiment is designed to search for any massive, stable or long-lived, slow-moving particle [5] with single or multiple electric charges that arise in various scenarios of physics beyond the Standard Model (SM). For an extended and detailed account of the MoEDAL discovery potential, the reader is referred to the *MoEDAL Physics Programme* [6]. Emphasis is given here on recent MoEDAL results, based on the exposure of magnetic monopole trapping volumes to 13 TeV proton-proton collisions.

The structure of this paper is as follows. Section 2 provides a description of the MoEDAL detector. Magnetic monopoles are briefly discussed in Section 3, while Section 4 presents the MoEDAL results on monopole searches. Section 5 is dedicated to prospects for MoEDAL to detect supersymmetric (meta)stable states. Planned extensions of the MoEDAL experiments are highlighted in Section 6. The paper concludes with a summary and an outlook in Section 7.

2. The MoEDAL detector

The MoEDAL detector [2] is deployed around the intersection region at Point 8 (IP8) of the LHC in the LHCb experiment Vertex Locator (VELO) [7] cavern. A three-dimensional depiction of the MoEDAL experiment is presented in Figure 1. It is a unique and largely passive LHC detector comprising four subdetector systems.
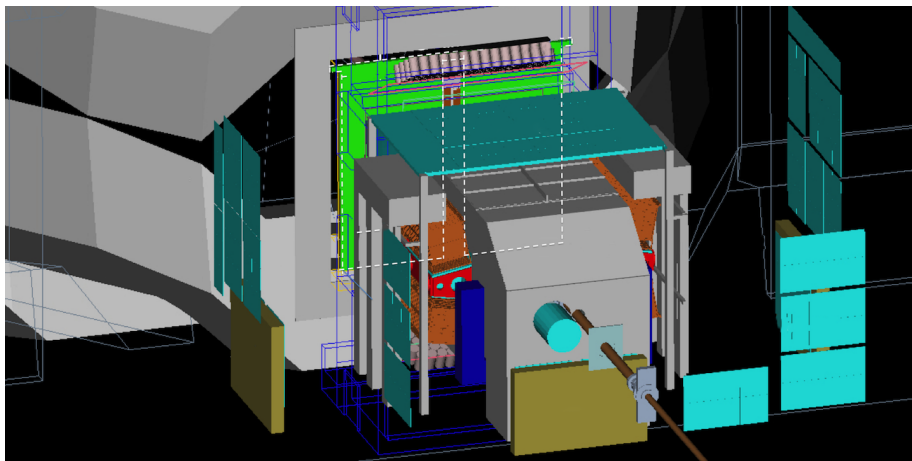
Figure 1: GEANT4 visualisation of the MoEDAL experiment around the LHCb VELO region at Point 8 of the LHC prepared with the Panoramix package.

2.1 Low-threshold nuclear track detectors

The main subdetector system is made of a large array of CR-39, Makrofol® and Lexan™ nuclear track detector (NTD) stacks surrounding the intersection area. The passage of a highly

ionising particle through the plastic detector is marked by an invisible damage zone along the trajectory. The damage zone is revealed as a cone-shaped etch-pit when the plastic detector is chemically etched. Then the sheets of plastics are scanned looking for aligned etch pits in multiple sheets. The MoEDAL NTDs have a threshold of $z/\beta \sim 5$, where z is the charge and $\beta = v/c$ the velocity of the incident particle. During proton-proton collision runs, the only source of known particles that are highly ionising enough to leave a track in MoEDAL NTDs are spallation products with range that is typically much less than the thickness of one sheet of the NTD stack. In that case the ionising signature will be that of a very low-energy electrically charged *stopped* particle. This signature is distinct to that of a *penetrating* electrically or magnetically charged particle that will usually traverse every sheet in a MoEDAL NTD stack, accurately demarcating a track that points back to the collision point with a resolution of ~ 1 cm. Part of the Run 2 NTD deployment on the wall of the cavern is visible in Figure 2.

Figure 2: Part of the Run 2 NTD deployment on the wall of the cavern.

Figure 3: The VHCC between RICH1 and TT installed for Run 2.

2.2 Very high-charge catcher

A feature of the Run 2 deployment is the installation of a high-threshold NTD array ($z/\beta \sim$ 50): the Very High Charge Catcher (VHCC). The VHCC subdetector, consisting of two flexible low-mass stacks of Makrofol® in an aluminium foil envelope, is deployed in the forward acceptance of the LHCb experiment between the LHCb RICH1 detector and the Trigger Tracker (TT), as shown in Figure 3. It is the only NTD (partly) covering the forward region, adding only $\sim 0.5\%$ to the LHCb material budget while enhancing considerably the overall geometrical coverage of MoEDAL NTDs.

2.3 Magnetic trappers

A unique feature of the MoEDAL detector is the use of paramagnetic magnetic monopole trappers (MMTs) to capture electrically and magnetically charged highly ionising particles. The aluminium absorbers of MMTs are subject to an analysis looking for magnetically charged particles

at a remote SQUID magnetometer facility [8, 9]. The search for the decays of long-lived electrically charged particles that are stopped in the trapping detectors will be carried out subsequently, as explained in Section 6.3.

A trapping detector prototype was exposed to 8 TeV proton-proton collisions for an integrated luminosity of 0.75 fb^{-1} in 2012. For the 2015 run at 13 TeV, the MMT was upgraded to an array consisting of 672 square aluminium bars with dimensions $19 \times 2.5 \times 2.5$ cm^3, shown in Figure 4. A total mass of $\sim$800 kg stacked in boxes was placed 1.62 m from the IP8 LHC interaction point under the beam pipe on the side opposite to the LHCb detector (forward MMT) and in front of the lateral walls (side MMTs), as shown in Figure 1. The latest results on searches for monopoles for the Run 2 configuration are presented in Section 4.
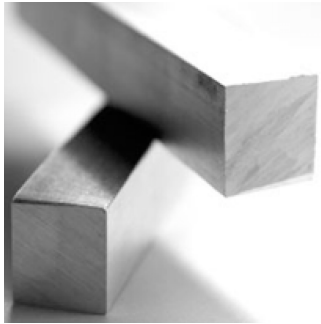
Figure 4: Sample of the MMT bars.
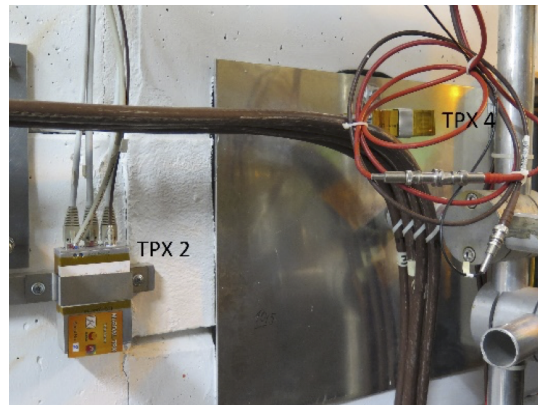
Figure 5: TimePix chips installed in MoEDAL.

2.4 TimePix radiation monitors

The only non-passive MoEDAL subdetector system comprises an array of TimePix pixel device arrays (256×256 square pixels with a pitch of 55 μm) distributed throughout the MoEDAL cavern at IP8, forming a real-time radiation monitoring system of highly ionising beam-related backgrounds. A photo of its readout setup for the 2015 installations is shown in Figure 5. Each pixel of the innovative TimePix chip comprises a preamplifier, a discriminator with threshold adjustment, synchronisation logic and a 14-bit counter. The operation of TimePix in time-over-threshold mode allows a 3D mapping of the charge spreading effect in the whole volume of the silicon sensor, thus differentiating between different types of particles species from mixed radiation fields and measuring their energy deposition [10].

3. Magnetic monopoles

The MoEDAL detector is designed to fully exploit the energy-loss mechanisms of magnetically charged particles [11 − 14] in order to optimise its potential to discover these messengers of new physics. There are various theoretical scenarios in which magnetic charge would be produced at the LHC [6]: (light) 't Hooft-Polyakov monopoles [13 − 15], electroweak monopoles [16 − 22], global monopoles [23 − 29] and monopolium [12, 30 − 32]. Magnetic monopoles that carry a

nonzero magnetic charge and dyons possessing both magnetic and electric charge [33] are among the most fascinating hypothetical particles. Even though there is no generally acknowledged empirical evidence for their existence, there are strong theoretical reasons to believe that they do exist, and they are predicted by many theories including grand unified theories and superstring theory [34, 35].

The theoretical motivation behind the introduction of magnetic monopoles is the symmetrisation of the Maxwell equations and the explanation of the charge quantisation [11]. Dirac showed that the mere existence of a monopole in the universe could offer an explanation of the discrete nature of the electric charge, leading to the Dirac Quantisation Condition (DQC),

$$\alpha g = \frac{N}{2} e, \quad N = 1, 2, ...,\tag{3.1}$$

where e is the electron charge, $\alpha = \frac{e^2}{4\pi\hbar c \varepsilon_0} = \frac{1}{137}$ is the fine structure constant (at zero energy, as appropriate to the fact that the DQC pertains to long (infrared) distances from the centre of the monopole), ε_0 is the vacuum permittivity, and g is the monopole magnetic charge. In Dirac's formulation, magnetic monopoles are assumed to exist as pointlike particles and quantum mechanical consistency conditions lead to Eq. (3.1), establishing the value of their magnetic charge. Although monopoles symmetrise Maxwell equations in form, there is a numerical asymmetry arising from the DQC, namely that the basic magnetic charge is much larger than the smallest electric charge. A magnetic monopole with a single Dirac charge g_D has an equivalent electric charge of $137e/2$. Thus for a relativistic monopole the energy loss is around 4,700 times (68.5^2) that of a minimum-ionising electrically charged particle. The monopole mass, as well as its spin, remains a free parameter of the theory.

3.1 Monopolium

A possible explanation for the lack of experimental confirmation of monopoles is Dirac's proposal [11, 12, 30] that monopoles are not seen freely because they form a bound state called *monopolium* [31, 32, 36, 37] being confined by strong magnetic forces. Monopolium is a neutral state, hence it is difficult to detect directly at a collider detector, although its decay into two photons would give a rather clear signal for the ATLAS and CMS detectors [38, 39], which however would not be visible in the MoEDAL detector. Other studies [40, 41] propose to exploit the scattering of charged particles off monopole-antimonopole pairs. Such techniques would be appealing for detecting monopolia at the LHC.

3.2 Monopole production at colliders

Direct monopole pair production in colliders can proceed via two processes: a Drell-Yan-like (DY) process in photon *s*-channel intermediation and a photon-fusion *t*-channel diagram. An important cautionary remark should be made here. In both cases, the monopole pair couples to the photon via a coupling that depends on g_D and hence it is $\mathcal{O}(10)$. This large monopole–photon coupling invalidates any perturbative treatment of the cross-section calculation and hence any result based on it is *only indicative* and used merely to facilitate comparisons between experiments. On the contrary, the upper bounds placed on production cross-sections are solid and can be relied upon [42].

This situation may be resolved if thermal Schwinger production of monopoles in heavy-ion collisions is considered [43]. This mechanism becomes effective in the presence of strong electromagnetic fields and does not rely on perturbation theory, therefore it overcomes these limitations [44 – 48].

Another possibility is the photon-fusion production for fermionic and vector boson monopoles when a β-dependent coupling[1] and a magnetic-moment term κ is considered [49]. The perturbativity is guaranteed when the discussion is limited to very slow ($\beta \ll 1$) monopoles, when $\kappa \to \infty$ and at the same time the following condition is met:

$$g\kappa\beta^2 < 1. \tag{3.2}$$

The cross-section remains finite at this limit for photon fusion while it vanishes for Drell-Yan. Such a treatment opens up the possibility to interpret the cross-section bounds set in collider experiments [50 – 52] in a proper way, thus yielding sensible monopole-mass limits.

4. Searches for monopoles in MoEDAL

The high ionisation of slow-moving magnetic monopoles and dyons, implies quite characteristic trajectories when such particles interact with the MoEDAL NTDs, which can be revealed during the etching process [2, 6]. In addition, the high magnetic charge of a monopole (which is expected to be at least one Dirac charge $g_D = 68.5e$ (cf. Eq. (3.1)) implies a strong magnetic dipole moment, which in turn may result in a strong binding of the monopole with the $^{27}_{13}$Al nuclei of the aluminium MoEDAL MMTs. In such a case, the presence of a monopole trapped in an aluminium bar of an MMT would be detected through the existence of a persistent current, defined as the difference between the currents in the SQUID of a magnetometer before and after the passage of the bar through the sensing coil.

The MoEDAL experiment published its first physics analysis paper in 2016 based on the MMT data taken at the collision energy of 8 TeV during 2012 in Run 1 [53]. Model-independent cross-section limits were obtained in fiducial regions of monopole energy and direction for $1g_D \leq |g| \leq 6g_D$. Since then it has released more MMT results from exposures to 13 TeV pp collisions in LHC Run 2 [54 – 56].

In its most recent search for monopoles, the MoEDAL Collaboration used data taken at a centre-of-mass energy of 13 TeV with a delivered integrated luminosity of 4.0 fb^{-1} [56]. In this search, the photon-fusion monopole production mechanism, characterised by much higher cross-section than DY at LHC energies [49], was considered for the first time at LHC when interpreting the results. Different monopole–photon couplings were assumed — β-independent and β-dependent —, different spins of monopole (spin 0, ½ and 1) and both Drell-Yan and photon-fusion production mechanisms. This interpretation used the results of a detailed phenomenological study which compared Drell-Yan and photon-fusion mechanisms for both assumptions of the photon–monopole coupling [49].

---

[1]The parameter β is defined by the Lorentz invariant expression $\beta = \sqrt{1 - \frac{4M^2}{s}}$, where M is the monopole mass and s is the Mandelstam variable for the initial-state particles.

In this analysis, the MoEDAL trapping detector, consisting of 794 kg of aluminium samples installed in the forward and lateral regions, was analysed by searching for induced persistent currents after passage through the SQUID magnetometer at ETH Zurich. As shown in Figure 6, the measurements were compatible with the absence of monopoles and therefore magnetic charges equal to or above the Dirac charge were excluded in all samples [56]. Cross-section upper limits as low as 11 fb were set, improving previous limits of 40 fb also set by MoEDAL [55]. Mass limits in the range 1500–3750 GeV were set for magnetic charges up to $5g_D$ for monopoles of spins 0, ½ and 1 — the strongest to date at a collider experiment [42] for charges ranging from three to five times the Dirac charge. For a comparison, previous DY mass limits set by MoEDAL at 13 TeV ranged from 450 to 1790 GeV [55]. Moreover, the MMT scanning results were interpreted recently in dyon production [57]; the first search for dyons in a collider experiment.

In Figure 7, cross-section upper limits at 95% confidence limit (CL) are shown for spin-½ monopoles and for various magnetic charges, together with the leading-order calculations for the photon-fusion and Drell-Yan mechanisms. The weaker limits for $|g| = g_D$, when compared to higher charges, are mostly due to loss of acceptance from monopoles punching through the trapping volume. For higher charges, monopoles ranging out before reaching the trapping volume decrease the acceptance for DY monopoles with increasing charge.
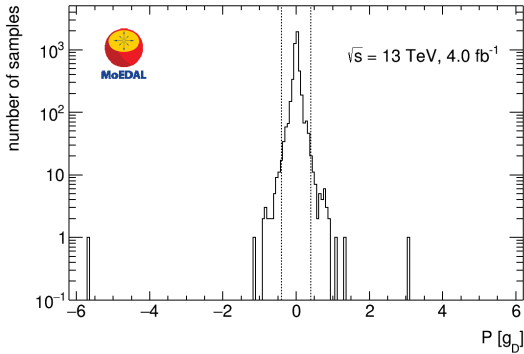
Figure 6: SQUID analysis results: Magnetic pole strength (in units of Dirac charge, g_D) measured through the induced persistent current in the 2400 aluminium samples of the MoEDAL trapping detectors exposed to 13 TeV pp collisions in 2015–2017 with every sample scanned twice [56].
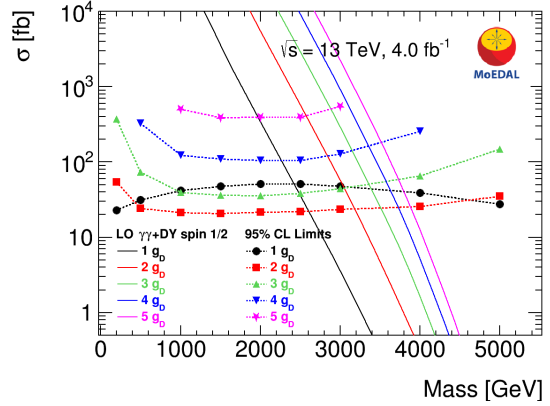
Figure 7: 95% CL cross-section upper limits for combined DY & $\gamma\gamma$ monopole pair production with β-independent coupling in 13 TeV pp collisions as a function of mass for spin-½ monopoles. The colours correspond to different charges. The solid lines are cross-section calculations at leading order [56].

Under the assumption of photon-fusion and Drell-Yan cross-sections, mass limits are derived for $1g_D \leq |g| \leq 5g_D$ by the MoEDAL experiment [56], complementing other results obtained by the ATLAS Collaboration [58–60], which placed limits for monopoles with magnetic charge $|g| \leq 2g_D$, as demonstrated in Figure 8. The ATLAS bounds are better that the MoEDAL ones for $|g| = 2g_D$ due to the higher luminosity delivered in ATLAS and the loss of acceptance in MoEDAL for small magnetic charges. On the other hand, higher charges are difficult to be probed in ATLAS due to the limitations of the electromagnetic-calorimeter-based level-1 trigger deployed for such searches [60]. A comparison of the limits on monopole production cross-sections set by other col-

liders with those set by MoEDAL is presented in Ref. [35], while general limits including searches in cosmic radiation are reviewed in Refs. [50, 52].
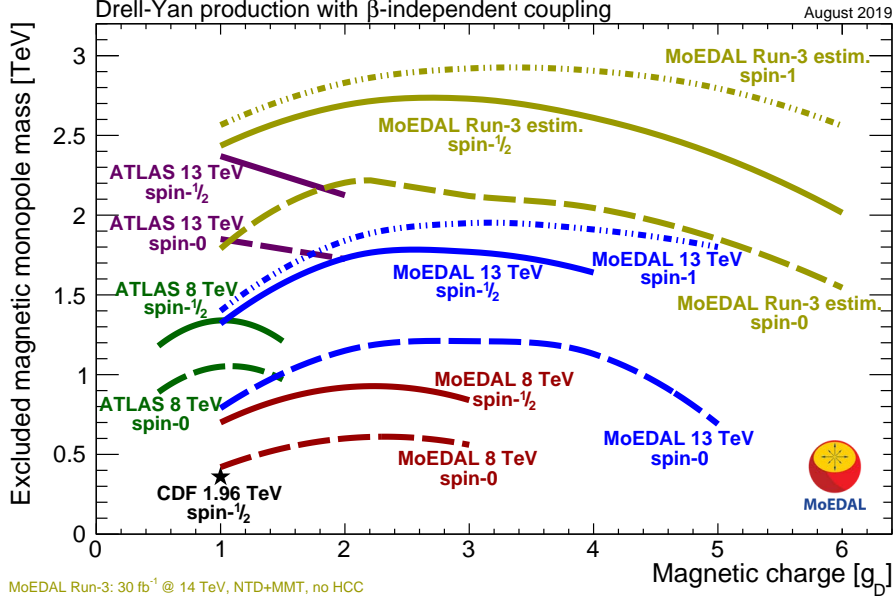
Figure 8: Magnetic monopole mass limits from CDF [61], ATLAS [59, 60] and MoEDAL searches [53, 56] as a function of magnetic charge for various spins, assuming a Drell-Yan pair-production mechanism and β-independent coupling.

5. Beyond magnetic monopoles: supersymmetry

The MoEDAL detector is also designed to search for any massive, long-lived, slow-moving particles [5, 62] with single or multiple electric charges arising in many scenarios of physics beyond the Standard Model. Supersymmetric long-lived particles [63 – 66], quirks, strangelets, Q-balls, and many others fall into this category [6]. A generic search for high-electric-charge objects is currently underway [67]. Here we focus on the possibility to discover supersymmetric signals with the MoEDAL NTDs.

Apart from the NTDs, MoEDAL can also exploit the exposure of MMTs, this time to capture heavy stable charged particles (HSCPs), which can only be observed through the detection of their decaying products. To this effect, the MoEDAL Apparatus for detecting extremely Long Lived particles, described in more detail in Section 6.3, is planned to be installed in a gallery in IP8 in Run 3.

Supersymmetry (SUSY) [68] is an extension of the Standard Model which assigns to each SM field a superpartner field with a spin differing by a half unit. SUSY provides elegant solutions to several open issues in the SM, such as the hierarchy problem, the identity of dark matter, and grand unification. SUSY scenarios propose a number of massive slowly moving electrically charged particles. If they are sufficiently long lived to travel a distance of at least $\mathscr{O}(1\,\text{m})$ before decaying and their $z/\beta \gtrsim 5$, then they may be detected in the MoEDAL NTDs. No highly charged particles are

expected in such a theory, but there are several scenarios in which supersymmetry may yield massive, long-lived particles that could have electric charges $\pm 1e$, potentially detectable in MoEDAL if they are produced with low velocities ($\beta \lesssim 0.2$) .

5.1 HSCPs & SUSY @ LHC

In supersymmetric models, various instances of sparticles/objects may emerge as HSCPs. Considering its detector placements in the cavern and its low-velocity sensitivity, MoEDAL may detect HSCPs with proper lifetimes $c\tau \gtrsim 1$ m.

Sleptons: They may be long-lived as next-to-the-lightest SUSY partners (NLSPs) decaying to a gravitino or a neutralino LSP. In gauge-mediated symmetry breaking (GMSB), the $\tilde{\tau}_1$ NLSP decays to $\tilde{G}$ may be suppressed due to the 'weak' gravitational interaction [69], remaining partly compatible with constraints on the dark-matter abundance in super-weakly interacting massive particle scenarios [70]. In other cases, such as the co-annihilation region in constrained MSSM, the most natural candidate for the NLSP is the lighter $\tilde{\tau}_1$, which could be long lived if the mass splitting between the $\tilde{\tau}_1$ and the $\tilde{\chi}_1^0$ is small [70 – 72]. This region is one of the most favoured by the measured dark-matter relic density [73].

R-hadrons: They are formed by hadronised metastable gluinos or squarks. Gluino R-hadrons arise in Split SUSY due to the ultra-heavy squarks strongly suppressing $\tilde{g}$ decays to $\tilde{q}$ and quarks [74, 75]. Other models, such as *R*-parity-violating (RPV) SUSY [76] or gravitino dark matter [77], could produce a long-lived squark ($\tilde{t}$ or $\tilde{b}$) that would also form an R-hadron.

Charginos: Their long lifetime may be due to their mass degeneracy with the $\tilde{\chi}_1^0$ LSP in anomaly-mediated symmetry breaking (AMSB) scenarios [78, 79]. When they decay within the detectors to a soft $\pi^{\pm}$ and a $\tilde{\chi}_1^0$, they manifest themselves as disappearing tracks [80, 81].

ATLAS and CMS have searched for stable sleptons, R-hadrons and charginos using anomalously high energy deposits in the silicon tracker and long time-of-flight measurements by the muon system. The (very recent) ATLAS analysis [82] has set the most stringent limits with 31.6 fb^{-1} of pp collisions at 13 TeV, while the CMS has used 2.5 fb^{-1} so far [83]. The ATLAS bounds at 95% CL are 2000 GeV for gluino R-hadrons, 1250 GeV for sbottom R-hadrons, 1340 GeV for stop R-hadrons, 430 GeV for sleptons and 1090 GeV for charginos with sufficiently long lifetime [82]. In Refs. [84, 85], summary plots of ATLAS and CMS analyses results pertaining to HSCPs are provided. For comprehensive and recent reviews on LHC past, current and future searches, the reader is referred to Refs. [51, 86].

5.2 Preliminary study on MoEDAL prospects

As discussed earlier, we concentrate our efforts on heavy long-lived sparticles with a large production cross section that, in addition, satisfy present bounds. Therefore, we do not only study the MoEDAL sensitivity, but we also contrast it with ATLAS/CMS expected results. The latter is achieved by making use of the CMS efficiencies for HSPCs published in Ref. [87], which were extracted in order to reinterpret previous HSCP search results by CMS [88] in specific supersymmetric models.

To model the MoEDAL detector response, we assume an NTD efficiency ε defined independently of the incident angle as

$$\varepsilon = \begin{cases} 1, & \beta \leq \beta_{\text{max}}, \\ 0, & \beta > \beta_{\text{max}}, \end{cases} \qquad \text{where } \beta_{\text{max}} = 0.1 \sim 0.2. \tag{5.1}$$

The geometrical coverage of the NTD is modelled by a 2 m radius sphere, although in reality some NTD panels are < 0.5 m away from the IP. To account for the non-hermetic NTD geometry, we considered the NTD coverage fraction in the azimuth ϕ as a function of pseudorapidity η. For the 2015 NTD deployment, this amounts to a geometrical acceptance of 18.7%.

We assume $\tilde{g}$ pair production, attempting to identify cascade decays of the $\tilde{g}$ to a $\tilde{\tau}_1$ which may evade the selection criteria applied in Ref. [88], hence weakening the exclusion limits set by CMS, while maintaining high MoEDAL efficiency, i.e. slow-moving staus. In particular, we focus on two of the selection cuts:

At least one Pixel hit: Requires the presence of a charged particle in the innermost part of the detector. The event may be rejected by the CMS analysis, if the $\tilde{g}$ decays via a long-lived neutral particle, e.g. a neutralino.

Small impact parameters $d_z, d_{xy} < 0.5$ **cm:** The long-lived charged track must point back to the primary vertex. It is imposed against cosmic-ray background. However, if a particle in the decay chain is long-lived and a kink is present, the event may be missed by CMS.

In the following, we require at least *two hits* in the NTDs to consider a parameter-space point as observable by MoEDAL, which represents a rather tight requirement, given the extremely low background expected. For CMS we only show 95% CL exclusion regions, which are typically more extensive than the discovery ones. In this respect, the comparison is rather biased favouring CMS, yet it serves well in the context of a preliminary study.

Concerning the datasets, we show projections for two LHC runs:

- **End of Run 2:** CMS has recorded ~ 150 fb^{-1} of *pp* collisions at $\sqrt{s} = 13$ TeV during 2015–2018, while MoEDAL was exposed to ~ 6.7 fb^{-1} at IP8.[2]

- **End of Run 3:** We assume a collision energy of $\sqrt{s} = 14$ TeV and 300 fb^{-1} for AT-LAS/CMS [89] to be collected during 2021–2023. The current scenario for LHCb is that it may receive roughly ten times less luminosity than ATLAS/CMS in Run 3, a significant improvement over Run 2 where this figure was ~ 50. Hence, we assume 30 fb^{-1} of delivered luminosity for MoEDAL by the end of 2023 [90].

The event analyses for MoEDAL and CMS have been carried out at parton level. In recasting the CMS analysis, we closely follow and use the recipe and efficiency maps provided in Ref. [87]. Several decay chains were tried; here we highlight one were the $\tilde{g}$ always decays to a $\tilde{\chi}_1^0$, which decays to a $\tilde{\tau}_1$ and a (heavy) τ. The mass splitting between the $\tilde{\chi}_1^0$ and the $\tilde{\tau}_1$ is fairly large (300 GeV),

---

[2]Due to the passive nature of the MoEDAL subsystems, the relevant integrated luminosity is the *delivered* rather than the recorded as in other experiments.

so the $\tilde{\chi}_1^0$ large lifetime is due to dynamical rather than kinematical reasons. Possibilities include an axino $\tilde{\chi}_1^0$ with a small coupling, or some vector-like fermion, which must be the neutral component of an $SU(2)$ doublet D' that enjoys $u_R^c Q D'$ and $\tau_R^c L D'$ couplings. The $\tilde{\chi}_1^0$ leaves no hit in the Pixel detector therefore the CMS efficiency suffers, while it does not affect the MoEDAL response. Moreover, the $\tilde{\tau}_1$ is produced with a kink, thus it does not point back to the IP, escaping detection by CMS due to the impact-parameter cuts. The reach comparison, shown in Figure 9, demonstrates clearly the effect of CMS missing a second cut: MoEDAL can improve significantly the sensitivity at large lifetimes.
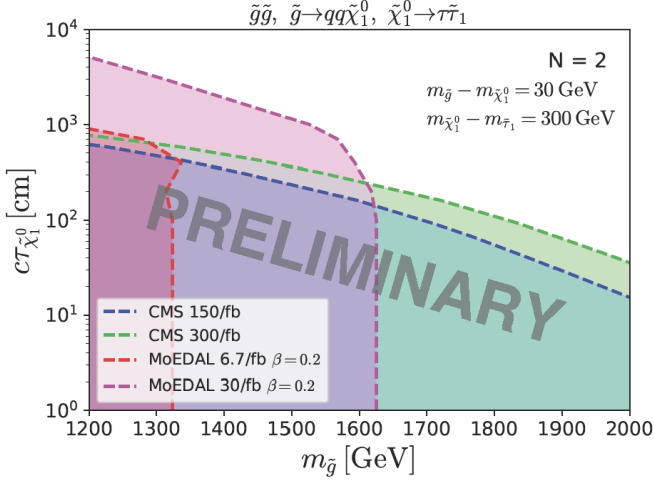
Figure 9: MoEDAL discovery reach requiring two signal events versus CMS 95% CL exclusion plot in the $\tilde{g}$ mass vs. $\tilde{\chi}_1^0$ lifetime plane for Run 2 (13 TeV) and for Run 3 (14 TeV) integrated luminosities. A scenario with gluino pair production where the $\tilde{g}$ decays to a long-lived $\tilde{\chi}_1^0$ decaying to a metastable $\tilde{\tau}_1$ and a τ is considered. The mass splitting between the $\tilde{\chi}_1^0$ and the $\tilde{g}$ ($\tilde{\tau}_1$) is 30 GeV (300 GeV). A $\tilde{\tau}_1$ detection threshold $z/\beta \geq 5 \Rightarrow \beta_{\max} = 0.2$ is assumed. From [65].

A word of caution is due here before drawing conclusions from this preliminary study:

1. We only considered one of the CMS analysis (similar for ATLAS), however other analyses sensitive to HSCPs might cover part or the whole of the region extended by MoEDAL, such as ones targeting displaced vertices [91 – 93] or disappearing tracks [80, 81]. Nonetheless, even in this case, the added value of MoEDAL would remain, since it provides a coverage with a completely different detector and analysis technique, thus with uncorrelated systematic uncertainties.

2. The ATLAS/CMS selection cuts applied here were optimised for 7 and 8 TeV data, which are not expected to be optimal for 13 and 14 TeV collisions. Besides that, further past (Run 2) and future (Run 3) improvements in the analysis have been or will be made, that have not been taken into account here.

3. In the MoEDAL analysis, we did not take into account the incident angle of the sleptons to the NTDs nor the presence of material in front of the NTDs. The former effect is taken into account in an updated study of the prospects for discovering supersymmetry with MoEDAL [66] in comparison with the latest ATLAS HSCP analysis [82].

Besides NTDs, another handle to probe SUSY LLPs can be provided by the MoEDAL Apparatus for Penetrating Particles, which is designed to search for millicharged particles and for new long-lived neutrals decaying to charged SM particles [94]. This subdetector, described in Sec-

tion 6.2, is expected to be sensitive to very delayed decays of neutral particles such as neutralinos in RPV scenarios [95, 96].

6. Future developments

The MoEDAL Collaboration plans to deepen and extend the discovery potential of the detector described in Section 2, by adding new subdetectors or by scanning material other than the MMTs exposed to LHC collisions. These developments are briefly described in this section.

6.1 CMS beam pipe

The induction technique has been successfully applied at the LHC with the dedicated MoEDAL trapping detector. Additional searches for trapped monopoles in beam-pipe material would access high values of magnetic charges and production cross sections to which other LHC experiments are insensitive [4]. The decommissioned central beam-pipe sections of ATLAS and CMS, with a 4π coverage and exposure to the highest rates of pp collisions, are the most attractive samples to be analysed.

The possibility of analysing decommissioned parts of the LHC beam-pipe system at the AT-LAS, CMS and LHCb/MoEDAL sites with a SQUID to search for trapped magnetic monopoles was proposed in 2017 through an expression of interest [97]. In this context, the MoEDAL experiment may serve as a formal platform for coordinating machining, scanning and analysis work, in collaboration with interested ATLAS, CMS and LHCb members. In February 2019, the CMS and MoEDAL collaborations signed an agreement transferring ownership of the Run-1 CMS beam pipe to MoEDAL. The 6 m long beryllium tube of 4 cm in diameter was cut into small pieces at the University of Alberta and scanned in the SQUID magnetometer at ETH Zurich during spring and summer of 2019. At present, simulation studies are underway to assess the acceptance of the beam pipe to monopole detection and the results are expected to be published soon.

6.2 MoEDAL Apparatus for Penetrating Particles

MoEDAL is proposing to deploy the MAPP (MoEDAL Apparatus for detecting Penetrating Particles) in the UGC1 gallery shielded by around 30 m of rock and concrete from the IP8 [94] and by an overburden of approximately 100 m of limestone from cosmic rays. It is envisaged that the first-stage detector, MAPP-1, a schematic view of which is given in Figure 10, will be installed during LS2 to take data in LHC Run 3. The purpose of the innermost detector, the *MAPP-mQP*, is to search for particles with fractional charge as small as $0.001e$, using scintillation bars. It will be made up of four collinear sections, with cross sectional area of 1.0 m^2, each comprised of 100 (10 cm $\times$ 10 cm) plastic scintillator bars each 75 cm long. A prototype of the mQP detector (10% of the original system) is already in place since 2017.

Another part of the detector, the *MAPP-LLP*, is deployed as three nested boxes of scintillator hodoscope detectors, in a 'Russian doll' configuration, following as far as possible the contours of the cavern. It is designed to be sensitive to long-lived neutral particles from new physics scenarios via their interaction or decay in flight in a decay zone of size approximately 5 m (wide) $\times$ 10 m (deep) $\times$ 3 m (high). The MAPP detector can be deployed in a number of positions ranging from 5°, at at distance of $\sim$ 55 m from IP8, to 25° at a distance of $\sim$ 25 m from IP8.

An upgrade plan for the MAPP-1 detector is envisaged for HL-LHC running from 2026 on, called MAPP-2. Currently, the concept is to extend the MAPP-LLP detector so as to occupy almost the whole UGC1 gallery.
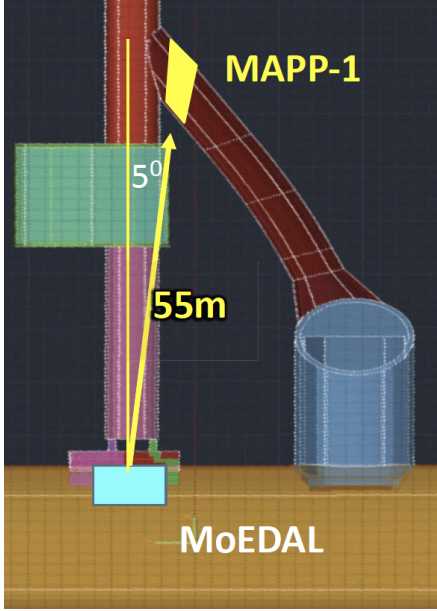
Figure 10: Planned positioning of the first phase of the MoEDAL MAPP subdetector, MAPP-1, in the UGC1 gallery, relative to the MoEDAL location as seen from above [98].

The MoEDAL-LLP detector should be sensitive to renormalisable portal interactions, leading to dark photons, dark Higgs bosons, heavy neutral leptons and other scenarios. In particular, dark Higgs bosons interact with the SM through a kinetic mixing term, thus probing one of the few possible renormalisable interactions with a hidden sector, the Higgs portal quartic scalar interaction [99]. Regarding their cosmological implications, dark Higgs bosons may mediate interactions with hidden dark matter that has the correct thermal relic density or resolves small-scale-structure discrepancies. A preliminary estimate of the projected sensitivity of MAPP-LLP with 30 and 300 fb^{-1} is illustrated in Figure 11. In this benchmark scenario, the (long-lived) dark Higgs ϕ mixes with SM H^0, leading to exotic $B \to X_s \phi$ decays with $\phi \to \ell^+ \ell^-$. The dark Higgs decay widths are suppressed by θ^2, where constraints on the mixing angle θ require $\sin\theta \simeq \theta \ll 1$. To facilitate comparison with other experiment sensitivities, a 100% tracking efficiency assumed with no background. Such scenarios will be probed by other planned LHC or beam-dump experiments [86]. Scenarios with heavy neutral leptons have also been examined [100], concluding that a heavy neutrino with a large enough electric dipole moment could in principle be detected at the LHC using MoEDAL's MAPP detector.

6.3 MoEDAL Apparatus for very Long Lived particles

MoEDAL is also planning another new subdetector called MALL (MoEDAL Apparatus for detecting extremely Long Lived particles) [94]. In this case MoEDAL trapping volumes, after they have been scanned through the ETH Zurich SQUID facility to identify any trapped monopole will be shipped to a remote underground facility to be monitored for the decay of pseudo-stable massive charged particles that may also have become trapped. MALL is the detector that monitors MoEDAL trapping volumes for decays of captured particles, the expected signal being the detection
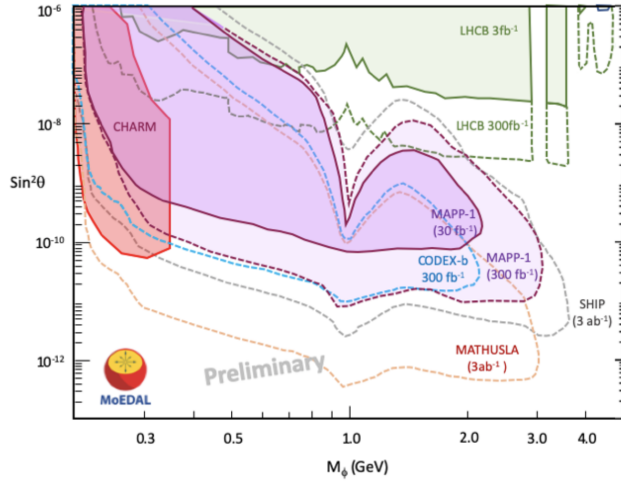
Figure 11: MAPP-LLP sensitivity with 30 and 300 fb^{-1} of pp collisions for a dark Higgs boson ϕ.

of at least one charged particle emanating from the monitored volume. The current plan is to place the MALL detector in the UGC1 gallery several metres from MAPP. The main background source will be cosmic rays, which is expected to be suppressed by using fast timing to determine the general direction of any track. A schematic view of the detector is shown in Figure 12. Initial estimates indicate that lifetimes up to around 10 yr can be probed. The MALL detector is designed to be sensitive to charged particles and to photons, with energy as small as 1 GeV. It is envisaged that construction of the detector will begin after the MAPP detector is full deployed.
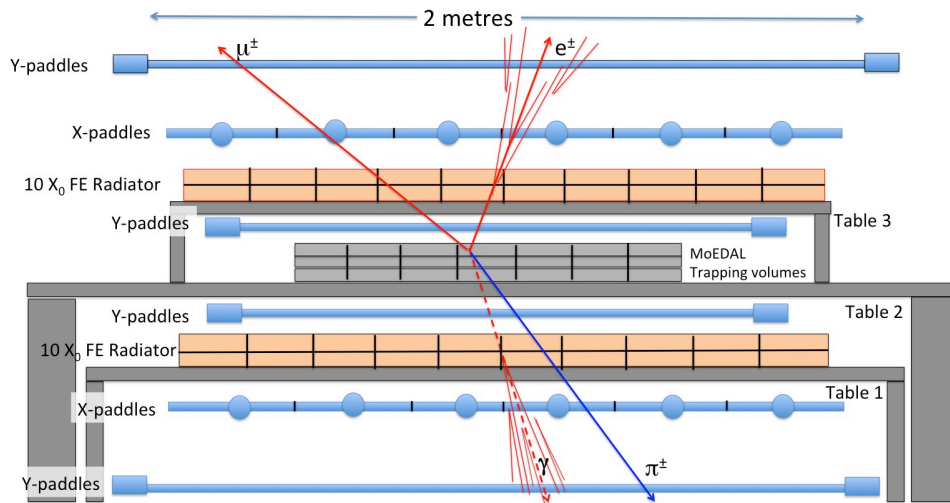
Figure 12: The MALL subdetector designed to monitor MoEDAL trapping volumes for the decays of trapped electrically charged particles with lifetimes as long as 10 years [94].

7. Summary and outlook

MoEDAL is extending considerably the LHC reach in the search for (meta)stable highly ionising particles. The latter are predicted in a variety of theoretical models and include: mag-

netic monopoles, SUSY long-lived spartners, D-matter [101 – 107], quirks, strangelets, Q-balls, etc [6, 63]. Such particles may be light enough to be producible at the LHC energies. In this paper we have described searches for monopoles and have discussed the MoEDAL relevance for long-lived partners in some SUSY models.

MoEDAL is optimised to probe precisely all such long-lived states, unlike the other LHC experiments [4]. Furthermore, it combines different detector technologies: plastic nuclear track detectors, trapping volumes and pixel sensors [2]. The first physics results, pertaining to magnetic monopole trapping detectors, obtained with LHC Run 1 data [53], and with 13 TeV *pp* collisions [54 – 56] have been published for monopoles and for dyons [57]. The MoEDAL Collaboration is preparing new analyses with more Run 2 data, with other detectors and with a large variety of interpretations involving not only magnetic but also electric charges [67].

In addition, MoEDAL is planning to install the MAPP and MALL upgrade detectors in the UGC1 gallery for Run 3. These two new detectors would allow MoEDAL's physics reach to be significantly expanded to include, in the case of the MAPP detector, the quest of millicharged and weakly interacting long-lived neutral particles. The MALL detector would allow the search for LLPs to be enlarged to include extremely long-lived charged particles.

Acknowledgments

References

[1] MoEDAL collaboration, "The MoEDAL experiment web page:." http://moedal.web.cern.ch/, 2020.

[2] MOEDAL collaboration, *Technical Design Report of the MoEDAL Experiment*, CERN-LHCC-2009-006, 2009.

[3] L. Evans and P. Bryant, *LHC machine*, *JINST* **3** (2008) S08001.

[4] A. De Roeck, A. Katre, P. Mermod, D. Milstead and T. Sloan, *Sensitivity of LHC Experiments to Exotic Highly Ionising Particles*, *Eur. Phys. J.* **C72** (2012) 1985 [1112.2999].

[5] M. Fairbairn, A. C. Kraan, D. A. Milstead, T. Sjostrand, P. Z. Skands and T. Sloan, *Stable massive particles at colliders*, *Phys. Rept.* **438** (2007) 1 [hep-ph/0611040].

[6] MOEDAL collaboration, *The Physics Programme of the MoEDAL Experiment at the LHC*, *Int. J. Mod. Phys.* **A29** (2014) 1430050 [1405.7662].

[7] LHCB collaboration, *The LHCb Detector at the LHC*, *JINST* **3** (2008) S08005.

[8] M. D. Joergensen, A. De Roeck, H. P. Hachler, A. Hirt, A. Katre, P. Mermod et al., *Searching for magnetic monopoles trapped in accelerator material at the Large Hadron Collider*, 1206.6793.

[9] A. De Roeck, H. P. Hachler, A. M. Hirt, M. D. Joergensen, A. Katre, P. Mermod et al., *Development of a magnetometer-based search strategy for stopped monopoles at the Large Hadron Collider*, *Eur. Phys. J.* **C72** (2012) 2212.

[10] B. Bergmann, P. Burian, P. Manek and S. Pospisil, *3D reconstruction of particle tracks in a 2 mm thick CdTe hybrid pixel detector*, *Eur. Phys. J.* **C79** (2019) 165.

[11] P. A. M. Dirac, *Quantised singularities in the electromagnetic field,*, *Proc. Roy. Soc. Lond.* **A133** (1931) 60.

[12] P. A. M. Dirac, *The Theory of magnetic poles*, *Phys. Rev.* **74** (1948) 817.

[13] G. 't Hooft, *Magnetic Monopoles in Unified Gauge Theories*, *Nucl. Phys.* **B79** (1974) 276.

[14] A. M. Polyakov, *Particle Spectrum in the Quantum Field Theory*, JETP Lett. **20** (1974) 194.

[15] V. Vento and V. Sari Mantovani, *On the magnetic monopole mass*, 1306.4213.

[16] Y. M. Cho and D. Maison, *Monopoles in Weinberg-Salam model*, *Phys. Lett.* **B391** (1997) 360 [hep-th/9601028].

[17] W. S. Bae and Y. M. Cho, *Finite energy electroweak dyon*, *J. Korean Phys. Soc.* **46** (2005) 791 [hep-th/0210299].

[18] Y. M. Cho, K. Kimm and J. H. Yoon, *Mass of the electroweak monopole*, *Mod. Phys. Lett.* **A31** (2016) 1650053 [1212.3885].

[19] Y. M. Cho, K. Kimm and J. H. Yoon, *Gravitationally coupled electroweak monopole*, *Phys. Lett.* **B761** (2016) 203 [1605.08129].

[20] J. Ellis, N. E. Mavromatos and T. You, *The price of an electroweak monopole*, *Phys. Lett.* **B756** (2016) 29 [1602.01745].

[21] J. Ellis, N. E. Mavromatos and T. You, *Light-by-light scattering constraint on Born-Infeld theory*, *Phys. Rev. Lett.* **118** (2017) 261802 [1703.08450].

[22] J. Alexandre and N. E. Mavromatos, *Weak-U(1) × strong-U(1) effective gauge field theories and electron-monopole scattering*, *Phys. Rev.* **D100** (2019) 096005 [1906.08738].

[23] M. Barriola and A. Vilenkin, *Gravitational Field of a Global Monopole*, *Phys. Rev. Lett.* **63** (1989) 341.

[24] A. K. Drukier and S. Nussinov, *Monopole Pair Creation in Energetic Collisions: Is It Possible?*, *Phys. Rev. Lett.* **49** (1982) 102.

[25] P. O. Mazur and J. Papavassiliou, *Gravitational scattering on a global monopole*, *Phys. Rev.* **D44** (1991) 1317.

[26] N. E. Mavromatos and J. Papavassiliou, *Singular lensing from the scattering on special space-time defects*, *Eur. Phys. J.* **C78** (2018) 68 [1712.03395].

[27] N. E. Mavromatos and S. Sarkar, *Magnetic monopoles from global monopoles in the presence of a Kalb-Ramond field*, *Phys. Rev.* **D95** (2017) 104025 [1607.01315].

[28] N. E. Mavromatos and S. Sarkar, *Regularized Kalb-Ramond magnetic monopole with finite energy*, *Phys. Rev.* **D97** (2018) 125010 [1804.01702].

[29] N. E. Mavromatos and S. Sarkar, *Finite-energy dressed string-inspired Dirac-like monopoles*, *Universe* **5** (2018) 8 [1812.00495].

[30] Ya. B. Zeldovich and M. Yu. Khlopov, *On the Concentration of Relic Magnetic Monopoles in the Universe*, *Phys. Lett.* **79B** (1978) 239.

[31] C. T. Hill, *Monopolonium*, *Nucl. Phys.* **B224** (1983) 469.

[32] V. K. Dubrovich, *Association of magnetic monopoles and antimonopoles in the early universe*, *Grav. Cosmol. Suppl.* **8N1** (2002) 122.

[33] J. S. Schwinger, *A Magnetic model of matter*, *Science* **165** (1969) 757.

[34] A. Rajantie, *Introduction to Magnetic Monopoles*, *Contemp. Phys.* **53** (2012) 195 [`1204.3077`].

[35] A. Rajantie, *The search for magnetic monopoles*, *Phys. Today* **69** (2016) 40.

[36] L. N. Epele, H. Fanchiotti, C. A. Garcia Canal and V. Vento, *Monopolium: The Key to monopoles*, *Eur. Phys. J.* **C56** (2008) 87 [`hep-ph/0701133`].

[37] L. N. Epele, H. Fanchiotti, C. A. G. Canal and V. Vento, *Monopolium production from photon fusion at the Large Hadron Collider*, *Eur. Phys. J.* **C62** (2009) 587 [`0809.0272`].

[38] L. N. Epele, H. Fanchiotti, C. A. G. Canal, V. A. Mitsou and V. Vento, *Looking for magnetic monopoles at LHC with diphoton events*, *Eur. Phys. J. Plus* **127** (2012) 60 [`1205.6120`].

[39] L. N. Epele, H. Fanchiotti, C. A. G. Canal, V. A. Mitsou and V. Vento, *Can the 750 GeV enhancement be a signal of light magnetic monopoles?*, `1607.05592`.

[40] V. Vento, *Ions, Protons, and Photons as Signatures of Monopoles*, *Universe* **4** (2018) 117.

[41] V. Vento and M. Traini, *Scattering of charged particles off monopole-antimonopole pairs*, *Eur. Phys. J.* **C80** (2020) 62 [`1909.03952`].

[42] PARTICLE DATA GROUP collaboration, *Review of Particle Physics*, *Phys. Rev.* **D98** (2018) 030001.

[43] J. S. Schwinger, *On gauge invariance and vacuum polarization*, *Phys. Rev.* **82** (1951) 664.

[44] O. Gould and A. Rajantie, *Magnetic monopole mass bounds from heavy ion collisions and neutron stars*, *Phys. Rev. Lett.* **119** (2017) 241601 [`1705.07052`].

[45] O. Gould and A. Rajantie, *Thermal Schwinger pair production at arbitrary coupling*, *Phys. Rev.* **D96** (2017) 076002 [`1704.04801`].

[46] O. Gould, S. Mangles, A. Rajantie, S. Rose and C. Xie, *Observing Thermal Schwinger Pair Production*, *Phys. Rev.* **A99** (2019) 052120 [`1812.04089`].

[47] O. Gould, D. L. J. Ho and A. Rajantie, *Towards Schwinger production of magnetic monopoles in heavy-ion collisions*, *Phys. Rev.* **D100** (2019) 015041 [`1902.04388`].

[48] D. L. J. Ho and A. Rajantie, *Classical production of 't Hooft-Polyakov monopoles from magnetic fields*, *Phys. Rev.* **D101** (2020) 055003 [`1911.06088`].

[49] S. Baines, N. E. Mavromatos, V. A. Mitsou, J. L. Pinfold and A. Santra, *Monopole production via photon fusion and Drell-Yan processes: MadGraph implementation and perturbativity via velocity-dependent coupling and magnetic moment as novel features*, *Eur. Phys. J.* **C78** (2018) 966 [`1808.08942`].

[50] L. Patrizii, Z. Sahnoun and V. Togo, *Searches for cosmic magnetic monopoles: past, present and future*, *Phil. Trans. Roy. Soc. Lond.* **A377** (2019) 20180328.

[51] L. Lee, C. Ohm, A. Soffer and T.-T. Yu, *Collider searches for long-lived particles beyond the Standard Model*, *Prog. Part. Nucl. Phys.* **106** (2019) 210 [`1810.12602`].

[52] N. E. Mavromatos and V. A. Mitsou, *Magnetic monopoles revisited: Models and searches at colliders and in the Cosmos*, `2005.05100`.

[53] MoEDAL Collaboration, *Search for magnetic monopoles with the MoEDAL prototype trapping detector in 8 TeV proton-proton collisions at the LHC*, *JHEP* **08** (2016) 067 [`1604.06645`].

[54] MoEDAL Collaboration, *Search for magnetic monopoles with the MoEDAL forward trapping detector in 13 TeV proton-proton collisions at the LHC*, *Phys. Rev. Lett.* **118** (2017) 061801 [`1611.06817`].

[55] MoEDAL collaboration, *Search for magnetic monopoles with the MoEDAL forward trapping detector in 2.11 fb^{-1} of 13 TeV proton-proton collisions at the LHC*, *Phys. Lett.* **B782** (2018) 510 [`1712.09849`].

[56] MoEDAL collaboration, *Magnetic monopole search with the full MoEDAL trapping detector in 13 TeV pp collisions interpreted in photon-fusion and Drell-Yan production*, *Phys. Rev. Lett.* **123** (2019) 021802 [`1903.08491`].

[57] MoEDAL collaboration, *First search for dyons with the full MoEDAL trapping detector in 13 TeV pp collisions*, `2002.00861`.

[58] ATLAS collaboration, *Search for magnetic monopoles in $\sqrt{s}$ =7 TeV pp collisions with the ATLAS detector*, *Phys. Rev. Lett.* **109** (2012) 261803 [`1207.6411`].

[59] ATLAS collaboration, *Search for magnetic monopoles and stable particles with high electric charges in 8 TeV pp collisions with the ATLAS detector*, *Phys. Rev.* **D93** (2016) 052009 [`1509.08059`].

[60] ATLAS collaboration, *Search for magnetic monopoles and stable high-electric-charge objects in 13 TeV proton-proton collisions with the ATLAS detector*, *Phys. Rev. Lett.* **124** (2020) 031802 [`1905.10130`].

[61] CDF collaboration, *Direct search for Dirac magnetic monopoles in p$\bar{p}$ collisions at $\sqrt{s}$ = 1.96 TeV*, *Phys. Rev. Lett.* **96** (2006) 201801 [`hep-ex/0509015`].

[62] S. Burdin, M. Fairbairn, P. Mermod, D. Milstead, J. Pinfold, T. Sloan et al., *Non-collider searches for stable massive particles*, *Phys. Rept.* **582** (2015) 1 [`1410.1374`].

[63] N. E. Mavromatos and V. A. Mitsou, *Physics reach of MoEDAL at LHC: magnetic monopoles, supersymmetry and beyond*, *EPJ Web Conf.* **164** (2017) 04001 [`1612.07012`].

[64] V. A. Mitsou, *Searches for New Physics with the MoEDAL detector at the LHC*, *PoS* **CORFU2017** (2018) 002.

[65] K. Sakurai, D. Felea, J. Mamuzic, N. E. Mavromatos, V. A. Mitsou, J. L. Pinfold et al., *SUSY discovery prospects with MoEDAL*, in *6th Symposium on Prospects in the Physics of Discrete Symmetries (DISCRETE 2018) Vienna, Austria, November 26-30, 2018*, 2019, `1903.11022`.

[66] D. Felea, J. Mamuzic, R. Maselek, N. E. Mavromatos, V. A. Mitsou, J. L. Pinfold et al., *Prospects for discovering supersymmetric long-lived particles with MoEDAL*, *Eur. Phys. J.* (2020) to appear [`2001.05980`].

[67] MoEDAL collaboration, *Search for high electrically charge objects and magnetic monopoles in 8 TeV pp collisions at the LHC using the full MoEDAL detector*, in preparation.

[68] J. Ellis, *Searching for supersymmetry and its avatars*, *Phil. Trans. Roy. Soc. Lond.* **A377** (2019) 20190069 [`1910.07489`].

[69] K. Hamaguchi, M. M. Nojiri and A. de Roeck, *Prospects to study a long-lived charged next lightest supersymmetric particle at the LHC*, *JHEP* **03** (2007) 046 [`hep-ph/0612060`].

[70] J. L. Feng, S. Iwamoto, Y. Shadmi and S. Tarem, *Long-lived sleptons at the LHC and a 100 TeV proton collider*, *JHEP* **12** (2015) 166 [`1505.02996`].

[71] T. Jittoh, J. Sato, T. Shimomura and M. Yamanaka, *Long life stau in the minimal supersymmetric standard model*, *Phys. Rev.* **D73** (2006) 055009 [`hep-ph/0512197`].

[72] S. Kaneko, J. Sato, T. Shimomura, O. Vives and M. Yamanaka, *Measuring lepton flavor violation at LHC with a long-lived slepton in the coannihilation region*, *Phys. Rev.* **D87** (2013) 039904 [`0811.0703`].

[73] J. R. Ellis, K. A. Olive, Y. Santoso and V. C. Spanos, *Supersymmetric dark matter in light of WMAP*, *Phys. Lett.* **B565** (2003) 176 [`hep-ph/0303043`].

[74] N. Arkani-Hamed and S. Dimopoulos, *Supersymmetric unification without low energy supersymmetry and signatures for fine-tuning at the LHC*, *JHEP* **06** (2005) 073 [`hep-th/0405159`].

[75] N. Arkani-Hamed, S. Dimopoulos, G. F. Giudice and A. Romanino, *Aspects of split supersymmetry*, *Nucl. Phys.* **B709** (2005) 3 [`hep-ph/0409232`].

[76] J. A. Evans and Y. Kats, *LHC coverage of RPV MSSM with light stops*, *JHEP* **04** (2013) 028 [`1209.0764`].

[77] J. L. Diaz-Cruz, J. R. Ellis, K. A. Olive and Y. Santoso, *On the feasibility of a stop NLSP in gravitino dark matter scenarios*, *JHEP* **05** (2007) 003 [`hep-ph/0701229`].

[78] G. F. Giudice, M. A. Luty, H. Murayama and R. Rattazzi, *Gaugino mass without singlets*, *JHEP* **12** (1998) 027 [`hep-ph/9810442`].

[79] L. Randall and R. Sundrum, *Out of this world supersymmetry breaking*, *Nucl. Phys.* **B557** (1999) 79 [`hep-th/9810155`].

[80] ATLAS collaboration, *Search for long-lived charginos based on a disappearing-track signature in pp collisions at $\sqrt{s} = 13$ TeV with the ATLAS detector*, *JHEP* **06** (2018) 022 [`1712.02118`].

[81] CMS collaboration, *Searches for physics beyond the standard model with the M_{T2} variable in hadronic final states with and without disappearing tracks in proton-proton collisions at $\sqrt{s} = 13$ TeV*, *Eur. Phys. J.* **C80** (2020) 3 [`1909.03460`].

[82] ATLAS collaboration, *Search for heavy charged long-lived particles in the ATLAS detector in 36.1 fb^{-1} of proton-proton collision data at $\sqrt{s} = 13$ TeV*, *Phys. Rev.* **D99** (2019) 092007 [`1902.01636`].

[83] CMS collaboration, *Search for long-lived charged particles in proton-proton collisions at $\sqrt{s} = 13$ TeV*, *Phys. Rev.* **D94** (2016) 112004 [`1609.08382`].

[84] ATLAS collaboration, "Summary plots from the ATLAS Supersymmetry physics group." https://atlas.web.cern.ch/Atlas/GROUPS/PHYSICS/CombinedSummaryPlots/SUSY/, 2020.

[85] CMS collaboration, "CMS Exotica Summary plots for 13 TeV data." https://twiki.cern.ch/twiki/bin/view/CMSPublic/SummaryPlotsEXO13TeV, 2020.

[86] J. Alimena et al., *Searching for long-lived particles beyond the Standard Model at the Large Hadron Collider*, `1903.04497`.

[87] CMS collaboration, *Constraints on the pMSSM, AMSB model and on other models from the search for long-lived charged particles in proton-proton collisions at sqrt(s) = 8 TeV*, *Eur. Phys. J.* **C75** (2015) 325 [`1502.02522`].

[88] CMS collaboration, *Searches for long-lived charged particles in pp collisions at $\sqrt{s}$ = 7 and 8 TeV*, *JHEP* **07** (2013) 122 [`1305.0491`].

[89] W. Walkowiak, *ATLAS plans for the high-luminosity LHC*, *PoS* **BEAUTY2018** (2018) 055.

[90] LHCʙ collaboration, *Prospects for searches for long-lived particles after the LHCb detector upgrades*, LHCb-CONF-2018-006, http://cds.cern.ch/record/2649825/, 2018.

[91] CMS collaboration, *Search for long-lived particles with displaced vertices in multijet events in proton-proton collisions at $\sqrt{s}$ = 13 TeV*, *Phys. Rev.* **D98** (2018) 092011 [`1808.03078`].

[92] ATLAS collaboration, *Search for displaced vertices of oppositely charged leptons from decays of long-lived particles in pp collisions at $\sqrt{s}$ = 13 TeV with the ATLAS detector*, *Phys. Lett.* **B801** (2020) 135114 [`1907.10037`].

[93] CMS collaboration, *Search for long-lived particles using nonprompt jets and missing transverse momentum with proton-proton collisions at $\sqrt{s}$ = 13 TeV*, *Phys. Lett.* **B797** (2019) 134876 [`1906.06441`].

[94] J. L. Pinfold, *The MoEDAL experiment: a new light on the high-energy frontier*, *Phil. Trans. Roy. Soc. Lond.* **A377** (2019) 20190382.

[95] D. Dercks, J. De Vries, H. K. Dreiner and Z. S. Wang, *R-parity violation and light neutralinos at CODEX-b, FASER, and MATHUSLA*, *Phys. Rev.* **D99** (2019) 055039 [`1810.03617`].

[96] D. Dercks, H. K. Dreiner, M. Hirsch and Z. S. Wang, *Long-lived fermions at AL3X*, *Phys. Rev.* **D99** (2019) 055020 [`1811.01995`].

[97] A. De Roeck, P. Mermod, J. Pinfold et al., *Searching for trapped magnetic monopoles in LHC accelerator material*, proposal, https://indico.cern.ch/event/623746/attachments/1427507/2190853/expression_of_interest_beam_pipe.pdf, 2017.

[98] M. Staelens, *Recent results and future plans of the MoEDAL experiment*, in *Meeting of the Division of Particles and Fields of the American Physical Society*, 10, 2019, `1910.05772`.

[99] B. Patt and F. Wilczek, *Higgs-field portal into hidden sectors*, `hep-ph/0605188`.

[100] M. Frank, M. de Montigny, P.-P. A. Ouimet, J. Pinfold, A. Shaa and M. Staelens, *Searching for heavy neutrinos with the MoEDAL-MAPP detector at the LHC*, *Phys. Lett.* **B802** (2020) 135204 [`1909.05216`].

[101] G. Shiu and L.-T. Wang, *D matter*, *Phys. Rev.* **D69** (2004) 126007 [`hep-ph/0311228`].

[102] J. R. Ellis, N. E. Mavromatos and D. V. Nanopoulos, *Time dependent vacuum energy induced by D particle recoil*, *Gen. Rel. Grav.* **32** (2000) 943 [`gr-qc/9810086`].

[103] J. R. Ellis, N. E. Mavromatos and D. V. Nanopoulos, *Derivation of a vacuum refractive index in a stringy space-time foam model*, *Phys. Lett.* **B665** (2008) 412 [`0804.3566`].

[104] J. R. Ellis, N. E. Mavromatos and M. Westmuckett, *A supersymmetric D-brane model of space-time foam*, *Phys. Rev.* **D70** (2004) 044036 [`gr-qc/0405066`].

[105] J. R. Ellis, N. E. Mavromatos and M. Westmuckett, *Potentials between D-branes in a supersymmetric model of space-time foam*, *Phys. Rev.* **D71** (2005) 106006 [`gr-qc/0501060`].

[106] N. E. Mavromatos, S. Sarkar and A. Vergou, *Stringy space-time foam, Finsler-like metrics and dark matter relics*, *Phys. Lett.* **B696** (2011) 300 [`1009.2880`].

[107] N. E. Mavromatos, V. A. Mitsou, S. Sarkar and A. Vergou, *Implications of a stochastic microscopic Finsler cosmology*, *Eur. Phys. J.* **C72** (2012) 1956 [`1012.4094`].